Soft Chemistry Synthesis and Characterization of Layered $Li_{1-x}Ni_{1-y}Co_yO_{2-\delta}$ ($0 \le x \le 1$ and $0 \le y \le 1$)

R. V. Chebiam, F. Prado, and A. Manthiram*

Materials Science and Engineering Program, ETC 9.104, The University of Texas at Austin, Austin, Texas 78712

Received March 19, 2001. Revised Manuscript Received June 18, 2001

$Li_{1-x}Ni_{1-y}Co_yO_{2-\delta}$ oxides have been synthesized for $0 \le x \le 1$ and $0 \le y \le 1$ by chemically extracting lithium at ambient temperature from $LiNi_{1-y}Co_yO_2$ with an oxidizing agent NO_2-PF_6 in acetonitrile medium. The samples have been characterized by X-ray diffraction, wet-chemical analyses to determine lithium and oxygen contents, and infrared spectroscopy. While the nickel-rich end members $Ni_{1-y}Co_yO_{2-\delta}$ have the O3 structure similar to the initial $LiNiO_2$, but with smaller lattice parameters, the cobalt-rich end members $Ni_{1-y}Co_yO_{2-\delta}$ consist of a mixture of P3 and O1 phases that are formed from the initial O3 structure of $LiCoO_2$ by a sliding of the oxide-ion layers. The nickel-rich phases $Li_{1-x}Ni_{1-y}Co_yO_{2-\delta}$ have an oxygen content close to 2 with a negligible amount of oxygen vacancies, while the cobalt-rich phases have considerable amount of oxygen vacancies ($\delta = 0.33$ in $CoO_{2-\delta}$). Fourier transform infrared spectroscopy indicates a semiconductor to metal transition in $Li_{1-x}CoO_{2-\delta}$ for $(1 - x) < 0.77$. On the other hand, $Li_{1-x}Ni_{1-y}Co_yO_{2-\delta}$ oxides with $0 \le y \le 0.5$ remain as semiconductors for the entire $0 \le (1 - x) \le 1$. The differences in oxygen loss behavior and electrical conduction are explained on the basis of qualitative band diagrams.

Introduction

The miniaturization and exponential growth of popular portable electronic devices such as laptop computers and cellular phones have created an ever-increasing demand for compact lightweight power sources. Lithium-ion batteries have become appealing in this regard as they offer higher cell voltage and energy density compared to other rechargeable systems. Commercial lithium-ion cells are commonly made with layered $LiCoO_2$ cathode and carbon anode. But cobalt is relatively toxic and expensive. Also, only 50% of the theoretical capacity of $LiCoO_2$, which corresponds to a reversible extraction of 0.5 lithium per Co, could be practically utilized (140 Ah/kg). These difficulties have created interest in alternate cathode hosts. In this regard, manganese oxides such as the spinel $LiMn_2O_4$[1] and layered $LiMnO_2$[2] have attracted much attention. However, the manganese oxides are confronted with a dissolution of manganese into the electrolyte particularly at higher temperatures and lattice distortions originating from the Jahn−Teller distortion associated with the high-spin Mn^{3+}:$3d^4$ ion. Additionally, the layered $Li_{1-x}MnO_2$ tends to transform to spinel-like phases during electrochemical charge/discharge cycling.[3] Recently, the cobalt substituted nickel oxides $LiNi_{1-y}Co_yO_2$ have drawn much attention as they offer much higher capacity (180 Ah/kg for $y = 0.15$ sample) than $LiCoO_2$.[4] This capacity corresponds to a reversible extraction of 0.65 lithium per transition metal ion. However, the structural and chemical stabilities of $Li_{1-x}Ni_{1-y}Co_yO_2$ at deep lithium extraction have not been fully assessed.

We recently investigated the structural stability under mild heat ($T > 50$ °C) of $Li_{1-x}Ni_{0.85}Co_{0.15}O_2$ samples that were obtained by chemical delithiation.[5] The results showed that the $Ni^{3+/4+}$ ions tend to migrate from the octahedral sites (3b sites) of the nickel planes to the octahedral sites (3a sites) of the lithium planes via the neighboring empty tetrahedral sites (6c sites). Such a migration was not found to occur in $Li_{1-x}CoO_2$ under similar conditions. The stability of the cobalt oxide is due to the strong octahedral site preference of low-spin $Co^{3+/4+}$ ions. Additionally, a substitution of about 30% cobalt for nickel in $Li_{1-x}Ni_{1-y}Co_yO_2$ was found to suppress such a cation migration. However, such a high content (30%) of Co lowers the practical capacity close to that of $LiCoO_2$.

With respect to the structural stability at ambient temperature, previous studies in the literature have focused mainly on samples obtained by an electrochemical extraction of lithium from $LiCoO_2$ and $LiNiO_2$.[6−13] The end member NiO_2 has generally been found to maintain the initial O3 structure (Figure 1) of $LiNiO_2$.[7−10] However, differences in the lithium-to-nickel ratio and cation ordering in the initial material before lithium extraction have been found to influence the structure of the end member NiO_2.While initial materials with small amounts of nickel in the lithium planes have been suggested to yield the O3 structure for the end member NiO_2, those with no nickel in the lithium planes have been found to yield the O1 structure for NiO_2;[10−12] the

(1) Thackeray, M. M.; David, W. I. F.; Bruce, P. G.; Goodenough, J. B. *Mater. Res. Bull.* **1983**, *18*, 461.
(2) Armstrong, A. R.; Bruce, P. G. *Nature* **1996**, *381*, 499.
(3) Vitins, G.; West, K. *J. Electrochem. Soc.* **1997**, *144*, 2587.
(4) Li, W.; Currie, J. C. *J. Electrochem. Soc.* **1997**, *144*, 2773.
(5) Chebiam, R. V.; Prado, F.; Manthiram, A. *J. Electrochem. Soc.* **2001**, *148*, A49.

10.1021/cm0102537 CCC: $20.00
Published on Web 08/29/2001

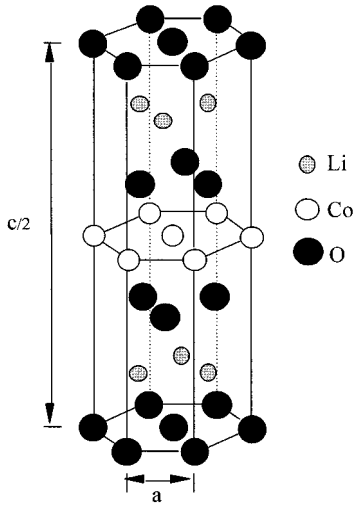

Figure 1. Crystal structure of $LiCoO_2$.

O1 structure is formed from the initial O3 structure by a sliding of oxygen layers. On the other hand, the end member CoO_2 has been generally found to have the O1 structure.[8,9,13] due to a sliding of oxygen layers during the lithium extraction process. However, not much attention has been paid to the chemical stability of the $LiNiO_2$ and $LiCoO_2$ phases during delithiation. For example, the variations of the oxidation state of the transition metal ions and the oxygen content with lithium content have not been monitored. The lack of such information is due to the difficulty of chemically determining the oxidation state and oxygen content with electrochemically prepared samples as they are contaminated with carbon, binder, and electrolyte. The objective of this paper is to synthesize $Li_{1-x}Ni_{1-y}Co_yO_2$ ($0 \le x \le 1$ and $0 \le y \le 1$) phases by chemically extracting lithium from the corresponding $LiNi_{1-y}Co_yO_2$ and monitor systematically the variation of oxygen content with lithium content. The $Li_{1-x}Ni_{1-y}Co_yO_2$ samples obtained by chemical delithiation are also characterized by X-ray diffraction and infrared spectroscopy to evaluate their structural stability during delithiation and electrical conduction behavior.

Experimental Section

The $LiNi_{1-y}Co_yO_2$ ($0 \le y \le 0.5$) samples were synthesized by a sol−gel procedure.[14] Required quantities of nickel acetate, cobalt acetate, and lithium carbonate (2 at. % excess) were dissolved in acetic acid, and the solution was refluxed. Small amounts of water and hydrogen peroxide were then added, and the solution was refluxed further until it became clear. The solution was then dried to produce a transparent gel, and the gel was decomposed at 400 °C for 10 min and then fired at 750 °C for 24 h in a flowing oxygen atmosphere. The $LiCoO_2$ sample was synthesized by a solid-state reaction of required quantities of lithium carbonate and cobalt oxide at 900 °C for 24 h in air.[15]

Chemical extraction of lithium from the $LiNi_{1-y}Co_yO_2$ samples was carried out by stirring the powders with an acetonitrile solution of the oxidizer NO_2PF_6 for 2 days under argon atmosphere:

$$LiNi_{1-y}Co_yO_2 + xNO_2PF_6 \rightarrow Li_{1-x}Ni_{1-y}Co_yO_2 + xNO_2 + xLiPF_6 \quad (1)$$

The products formed were filtered and washed repeatedly with acetonitrile under argon atmosphere to remove $LiPF_6$. The lithium contents before and after the lithium extraction reactions were determined by atomic absorption spectroscopy. The initial samples were found to have lithium contents of 1.00−1.02. The oxidation state of the transition metal ions and the oxygen content were determined by a redox (iodometric) titration.[16] Crystal chemical characterizations were carried out with X-ray powder diffraction using Cu Kα radiation. The lattice parameters were refined by the Rietveld method with the DBWS-9411 PC program.[17] Fourier transform infrared (FTIR) spectra were recorded with pellets made with KBr and the sample.

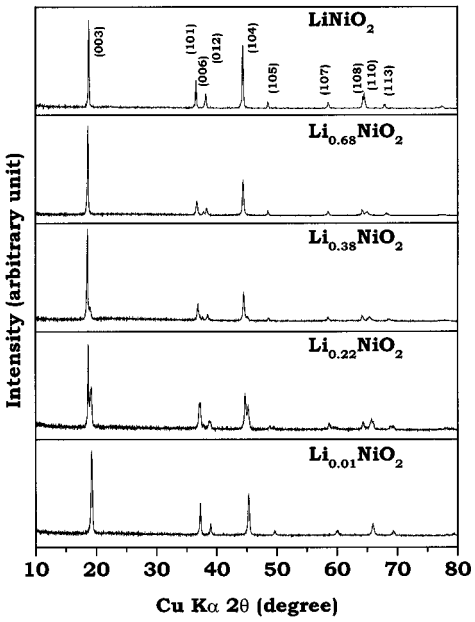

Figure 2. X-ray diffraction patterns of $Li_{1-x}NiO_2$.

Results and Discussion

Crystal Chemistry. Figures 2−4 show the X-ray diffraction patterns of $Li_{1-x}Ni_{1-y}Co_yO_2$ for $y = 0$, 0.15, and 1. In the case of $y = 0$ sample, the initial O3 structure (Figure 1) of $LiNiO_2$ that has an oxygen-stacking sequence of ABCABC along the *c*-axis like $CdCl_2$ is maintained for $0.4 \le (1 - x) \le 1$ (Figure 2). For $(1 - x) < 0.4$, a second phase begins to form as indicated by the appearance of a shoulder on the right-hand side of the (003) reflection centered at around 2θ

(6) Reimers, J. R.; Dahn, J. R. *J. Electrochem. Soc.* **1992**, *139*, 2091.
(7) Ohzuku, T.; Ueda, A.; Nagayama, M. *J. Electrochem. Soc.* **1993**, *140*, 1862.
(8) Amatucci, G. G.; Tarascon, J. M.; Klein, L. C. *J. Electrochem. Soc.* **1996**, *143*, 1114.
(9) Yang, X. Q.; Sun, X.; McBreen, J. *Electrochem. Commun.* **2000**, *2*, 100.
(10) Croguennec, L.; Pouillerie, C.; Delmas, C. *J. Electrochem. Soc.* **2000**, *147*, 1314.
(11) Arai, H.; Sakurai, Y. *Mater. Res. Soc. Symp. Proc.* **2000**, *575*, 3.
(12) Croguennec, L.; Pouillerie, C.; Mansour, A. N.; Delmas, C. J. *Mater. Chem.* **2001**, *11*, 131.
(13) Tarascon, J. M.; Vaughan, G.; Chabre, Y.; Seguin, L.; Anne, M.; Strobel, P.; Amatucci, G. *J. Solid State Chem.* **1999**, *147*, 410.
(14) Armstrong, T.; Prado, F.; Xia, Y.; Manthiram, A. *J. Electrochem. Soc.* **2000**, *147*, 435.
(15) Manthiram, A.; Chebiam, R. In *Ceramic Transactions: Processing and Characterization of Electrochemical Materials and Devices* ; Kumta, P. N., Manthiram, A., Sundaram, S. K., Chiang, Y. M., Eds.; American Ceramic Society: Westerville, OH, 1999; Vol. 109, p 277.
(16) Manthiram, A.; Swinnea, S.; Siu, Z. T.; Steinfink, H.; Goodenough, J. B. *J. Am. Chem. Soc.* **1987**, *109*, 6667.
(17) Young, R. A.; Shakthivel, A.; Moss, T. S.; Paiva Santos, C. O. *J. Appl. Crystallogr.* **1995**, *28*, 366.

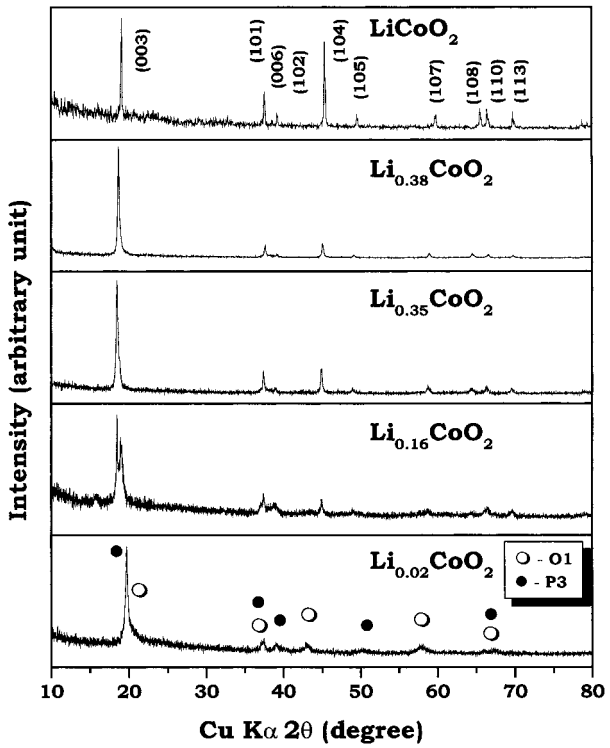

Figure 3. X-ray diffraction patterns of $Li_{1-x}CoO_2$.

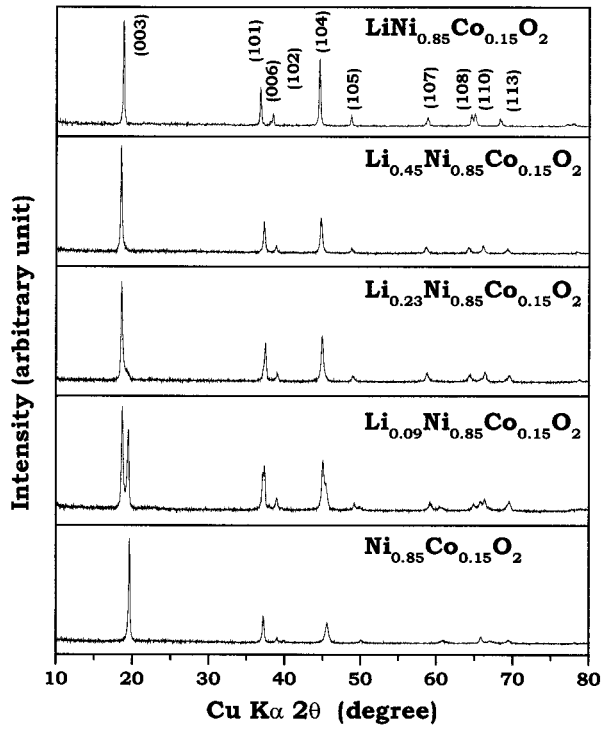

Figure 4. X-ray diffraction patterns of $Li_{1-x}Ni_{0.85}Co_{0.15}O_2$.

= 20°. The intensity of this new reflection increases with further decrease in lithium content, and the end member NiO_2 shows reflections corresponding to only the new phase. The crystal structure of the new phase could also be refined on the basis of the O3 structure (Figure 5a) but with smaller lattice parameters compared to the initial O3 phase. This refinement based on the rhombohedral $R\bar{3}m$ space group (S.G. 166) with nickel and cobalt ions in the 3b sites and oxide ions in the 6c sites yielded an R_{wp} of 9.57%. While $LiNiO_2$ has lattice

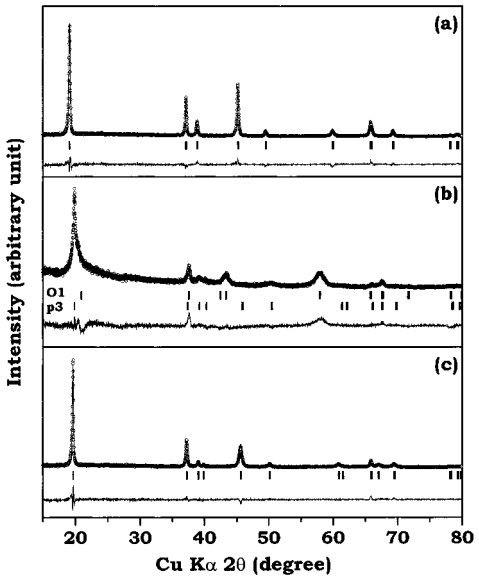

Figure 5. Rietveld refinement of the X-ray diffraction data of the end members (a) $NiO_{2-\delta}$, (b) $CoO_{2-\delta}$, and (c) $Ni_{0.85}Co_{0.15}O_{2-\delta}$. Circles and lines correspond to the observed and calculated diffraction data, respectively. The differences between the observed and calculated patterns are also shown.

parameters of $a = 2.886(1)$ and $c = 14.222(1)$ Å, NiO_2 has $a = 2.833(1)$ and $c = 13.870(1)$ Å. Thus a two-phase region consisting of two O3 phases exists for $0 < (1 - x) < 0.4$. In view of the previous literature reports,[10−12] the observation of the O3 structure for the chemically prepared NiO_2 suggests that a small amount of nickel could be present in the lithium plane in our initial material $LiNiO_2$. However, chemical analysis of our initial material indicated the lithium content to be 1.00. Additionally, we could not detect any nickel in the lithium plane by Rietveld refinement.

Figure 3 shows the X-ray diffraction patterns of the $Li_{1-x}CoO_2$ ($y = 1$) samples. In this case, the initial O3 structure is maintained for $0.35 \leq (1 - x) \leq 1$, and the new reflection on the right-hand side of the (003) peak begins to form for $(1 - x) < 0.35$. The intensity of the new reflection increases with further decrease in lithium content, and the end member CoO_2 shows reflections corresponding to only the new phase. The X-ray diffraction pattern of the new phase was analyzed using the Rietveld method on the basis of several models. Models based on (i) a single O1 phase, (ii) a mixture of two O1 phases, and (iii) a mixture of an O3 and an O1 phases could not account for the X-ray data satisfactorily. On the other hand, the crystal structure of the end member CoO_2 could be refined on the basis of a two-phase mixture consisting of a major P3 phase having lattice parameters of 2.827(1) and 13.445(1) Å and a minor O1 phase (CdI_2 structure) having lattice parameters of 2.772(1) and 4.263(1) Å (Figure 5b). A few weak reflections (for example, at around $2\theta = 40$ and 50°) present in Figure 5b could be accounted for only by the incorporation of a P3 phase in the refinement. The P3 structure was based on $R3m$ space group (S.G. 160) with cobalt ions at the 3a site (0,0,0) and oxide ions also at the 3a sites (0, 0, z) and (0, 0, z'), where z and z' are 0.5905 and 0.3764, respectively. The O1 structure was based on $P\bar{3}m1$ space group (S.G. 164) with cobalt ions at the 1a site (0,0,0) and oxide ions at the 2d sites (1/3,

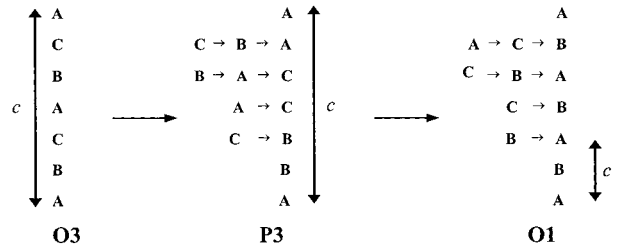

Figure 6. Schematics of the sliding of the oxide-ion layers illustrating the transformation of the O3 structure to P3 and O1 structures.

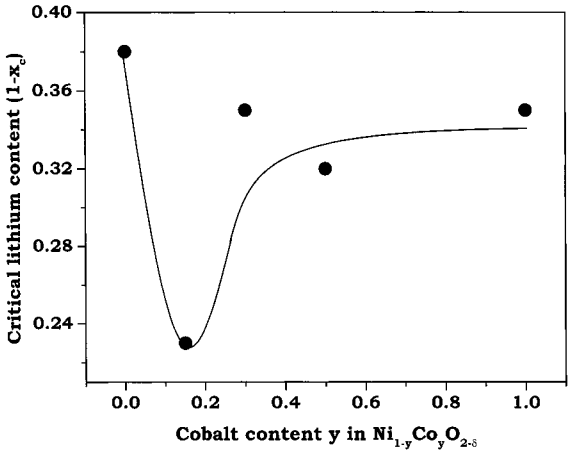

Figure 7. Variation of the critical value of the lithium content $(1 - x_c)$ at which the second phase begins to appear as a function of cobalt content y in$_{-x}Ni_{1-y}Co_yO_2$. The line provides a guide to the eye.

2/3, *z*), where $z = 0.248$. The poor crystallinity of the delithiated sample in Figure 5b and the presence of two phases resulted in a R_{wp} of 12.62%. The P3 and O1 phases have oxygen-stacking sequences of ABBCCA and ABAB, respectively, and they are formed from the initial O3 structure by a sliding of the oxide-ion layers as illustrated in Figure 6. The observation of the formation of a mixture of P3 and O1 phases for the chemically prepared CoO_2 sample is in contrast to the single O1 structure reported for the electrochemically prepared CoO_2.[8,9] The difference could be due to the differences in the degree of sliding during the electrochemical and chemical delithiation processes.

Figure 4 shows the X-ray diffraction patterns of the $Li_{1-x}Ni_{0.85}Co_{0.15}O_2$ ($y = 0.15$) samples. In this case, the initial O3 structure is maintained for a wider lithium content $0.23 \leq (1 - x) \leq 1$ and the new reflection on the right-hand side of the (003) peak begins to form at a lower lithium content $(1 - x) \leq 0.23$ compared to that in both $Li_{1-x}NiO_2$ (Figure 2) and $Li_{1-x}CoO_2$ (Figure 3). The crystal structure of the end member $Ni_{0.85}Co_{0.15}O_2$ could also be refined on the basis of the O3 structure (Figure 5c) similar to NiO_2. The refinement based on $R\bar{3}m$ space group (S.G. 166) yielded an R_{wp} of 10.97%. The end member $Ni_{0.85}Co_{0.15}O_2$ again has smaller lattice parameters ($a = 2.835(1)$ and c = 13.573(1) Å) as we found for NiO_2 compared to the initial O3 phase of $LiNi_{0.85}Co_{0.15}O_2$ ($a = 2.870(1)$ and $c = 14.196(1)$ Å). Figure 7 shows a plot of the critical lithium content $(1 - x_c)$ below which the second phase begins to form versus the cobalt content *y* in $Li_{1-x}Ni_{1-y}Co_yO_2$. The data show a minimum in $(1 - x_c)$ for $y = 0.15$. In other words, the $y = 0.15$ composition maintains the initial structure

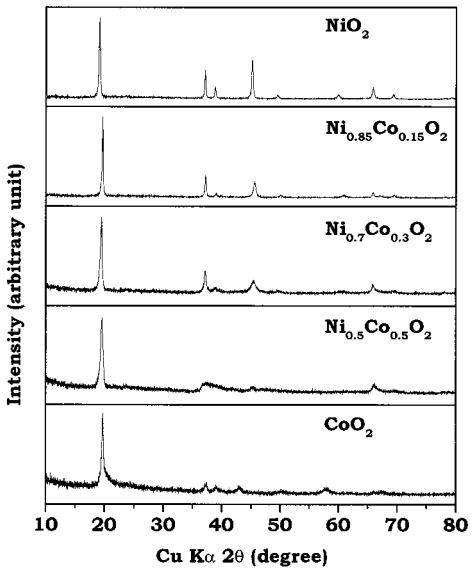

Figure 8. X-ray diffraction patterns of the end members $Ni_{1-y}Co_yO_{2-\delta}$.

to lower lithium contents, which could be one of the reasons for the higher electrochemical capacity observed for this composition compared to that found for $LiCoO_2$.

Figure 8 compares the X-ray diffraction patterns of the end members $Ni_{1-y}Co_yO_2$ for $0 \leq y \leq 1$. The reflections tend to become broader as the cobalt content increases, indicating poor crystallinity. Rietveld analysis (Figure 5) of the X-ray data of the end members reveal that the O3 structure is maintained for $0 \leq y \leq 0.3$. With further increase in the cobalt content *y*, the O3 structure is slowly destroyed, resulting in an ultimate mixture of P3 and O1 phases for the $y = 1$ sample. Thus the nickel-rich phases maintain the O3 structure, while the cobalt-rich phases do not. The crystallinity of the intermediate compositions with $y \approx 0.5$ are so poor that their X-ray diffraction data could not provide satisfactory structural information.

Oxygen Content. Figure 9 shows the variation of the oxidation state of the transition metal ions and the oxygen content with lithium content $(1 - x)$ in $Li_{1-x}Ni_{1-y}Co_yO_{2-\delta}$.In the case of $y = 0$ samples ($Li_{1-x}NiO_{2-\delta}$), the oxidation state of nickel increases proportionately with decreasing lithium content $(1 - x)$ as one would anticipate and the oxygen content remains close to 2. In contrast, in the case of $y = 1$ samples ($Li_{1-x}CoO_{2-\delta}$), the oxidation state of cobalt increases initially to about 3.35+ at around $(1 - x) = 0.65$ and remains constant thereafter. The constancy of the cobalt oxidation state at low lithium contents is reflected in a loss of oxygen from the lattice as indicated by a decrease in oxygen content below 2. The end member $CoO_{2-\delta}$ has an oxidation state of 3.34+ with $\delta = 0.33$. The observed loss of oxygen from the cobalt oxide system is in agreement with earlier results found for samples obtained by acid delithiation and chlorine oxidation.[18] Additionally, Tarascon et al.[13] have also suggested the presence of some oxygen vacancies in $CoO_{2-\delta}$ as they could obtain a better fit for the in-situ synchrotron data by assuming two O1 phases for the composition $CoO_{2-\delta}$

(18) Gupta, R.; Manthiram, A. *J. of Solid State Chem.* **1996**, *121*, 483.

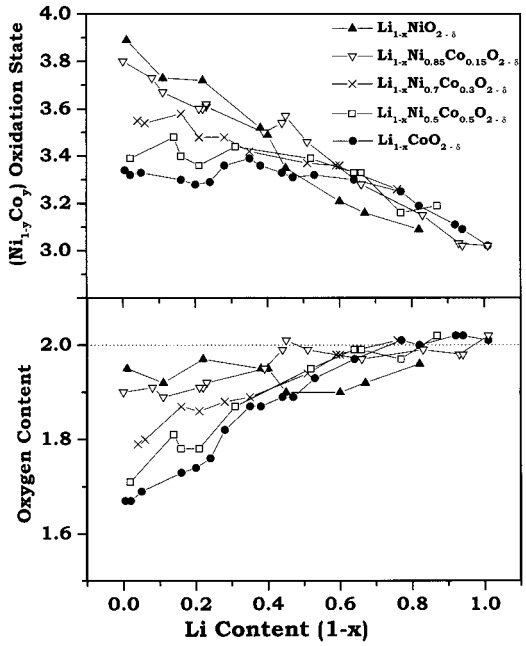

Figure 9. Variations of the oxidation state and oxygen content with lithium content in $Li_{1-x}Ni_{1-y}Co_yO_{2-\delta}$ for various cobalt contents *y*.

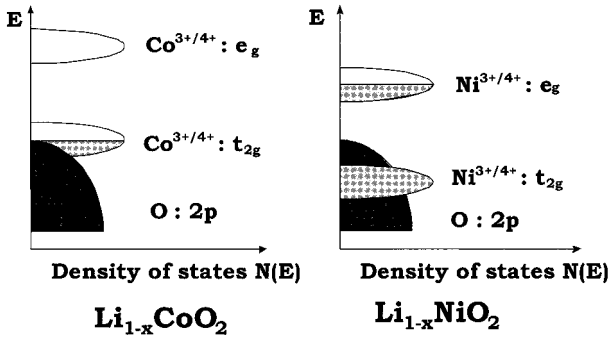

Figure 10. Comparison of the qualitative energy diagrams of $Li_{1-x}CoO_2$ and $Li_{1-x}NiO_2$.

with one of them having oxygen deficiency. The other compositions with $0 < y < 1$ show behaviors intermediate between those of $Li_{1-x}NiO_{2-\delta}$ and $Li_{1-x}CoO_{2-\delta}$. For a given lithium content $(1 - x)$, the oxidation state and oxygen content decrease with increasing cobalt content y in $Li_{1-x}Ni_{1-y}Co_yO_{2-\delta}$.

The differences in the variations of oxidation state and oxygen content with cobalt content *y* can be understood by considering the electronic structures. Figure 10 compares the qualitative band diagrams of the $y = 0$ and 1 systems, viz., $Li_{1-x}NiO_2$ and $Li_{1-x}CoO_2$.[19] In the case of $LiCoO_2$ with a Co^{3+}:$3d^6$ configuration, the t_{2g} band is completely filled and the e_g band is empty. As lithium is extracted from $LiCoO_2$, the Co^{3+} ions are oxidized to Co^{4+}, which is accompanied by a removal of electrons from the t_{2g} band. Since the t_{2g} band lies close to the top of the O:2p band, deeper lithium extraction with $(1 - x) < 0.5$ results in a removal of electrons from the O:2p band as well. The removal of a significant amount of electrons from the O:2p band will result in an oxidation of O^{2-} ions and an ultimate loss of oxygen from the lattice. In contrast, the $LiNiO_2$ system with a Ni^{3+}:$3d^7$ configuration involves removal of electrons only from the e_g band. Since the e_g band lies well above the O:2p band, $Li_{1-x}NiO_2$ does not lose oxygen down to a lower lithium content. As cobalt is substituted for nickel, the concentration of electrons in the e_g band decreases, leading to a removal of electrons from the t_{2g} band and a loss of oxygen at low lithium contents.

The band diagram for the cobalt oxide system and the observed oxygen loss are consistent with the recent X-ray absorption spectroscopic[20] and electron energy loss spectroscopic data.[21] The spectroscopic data indicate that the holes are introduced into the O:2p band rather than into the Co:3d band during the electrochemical extraction of lithium. Introduction of significant amount of holes into the O:2p band will result in an oxidation of O^{2-} ions and an ultimate evolution of oxygen from the lattice. Similarly, the negligible amount of oxygen loss in the nickel-rich compositions is consistent with an in-situ X-ray absorption spectroscopic (XAS) data of $Li_{1-x-z}Ni_{1+z}O_2$[22] and X-ray near-edge absorption spectroscopic (XANES) data of $Li_{1-x}Ni_{0.85}Co_{0.15}O_2$.[23] The spectroscopic data show a monotonic increase in the oxidation state of nickel on extracting lithium.

It is clear that the cobalt-rich phases experience a greater chemical instability with respect to oxygen loss on deep lithium extraction (charging) compared to the nickel-rich phases. The tendency to lose oxygen at deep lithium extraction appears to limit the practical capacity of $Li_{1-x}CoO_2$ to 140 mAh/g, which corresponds to a reversible extraction of 0.5 lithium per cobalt. On the other hand, the resistance of $Li_{1-x}Ni_{0.85}Co_{0.15}O_2$ to lose oxygen at deep lithium extraction and the formation of the second phase at a much lower lithium content $(1-x) < 0.23$ (Figure 4) lead to the realization of a much higher practical capacity of 180 mAh/g, which corresponds to a reversible extraction of 0.65 lithium per transition metal ion.

The differences in oxygen loss behavior may also explain the differences in the crystal chemistry of the end members $Ni_{1-y}Co_yO_{2-\delta}$. The P3 structure found in the case of cobalt-rich phases involves the presence of oxide ions directly above one another, and, therefore, it is generally formed with larger cations such as as Na^+ and K^+; it has never been reported for $Li_{1-x}MO_2$ phases before. However, for a given alkali metal ion, the formation of P3 structures is favored by decreasing the alkali metal content $(1 - x)$ in $A_{1-x}CoO_2$ (A = Na or K).[24] We believe the presence of a large amount of oxygen vacancies in $CoO_{2-\delta}$ along with the presence of little or no lithium in it reduces the repulsion between the oxide ion layers and makes the formation of the P3 phase possible. Thus, the formation of a significant amount of oxygen vacancies at deep lithium extraction may introduce structural instability and cause a sliding of the oxide-ion layers, as shown in Figure 6. In contrast,

(19) Chebiam, R. V.; Prado, F.; Manthiram, A. *Electrochem. Solid State Lett.*, submitted for publication.

(20) Montoro, L. A.; Abbate, M.; Rosolen, J. M. *Electrochem. Solid State Lett.* **2000**, *3*, 410.

(21) Hightower, A.; Graetz, J.; Ahn, C. C.; Rez, P.; Fultz, B. 198th Meeting of the Electrochemical Society, Phoenix, AZ, Oct 22−27, 2000, Abstract No. 177.

(22) Mansour, A. N.; Yang, X. Q.; Sun, X.; McBreen, J.; Croguennec, L.; Delmas, C. *J. Electrochem. Soc.* **2000**, *147*, 2104.

(23) Balasubramanian, M.; Sun, X.; Yang, X. Q.; McBreen, J. *J. Electrochem. Soc.* **2000**, *147*, 2903.

(24) Delmas, C.; Fouassier, C.; Hagenmuller P. *Physica B* **1980,** *99*, 81.

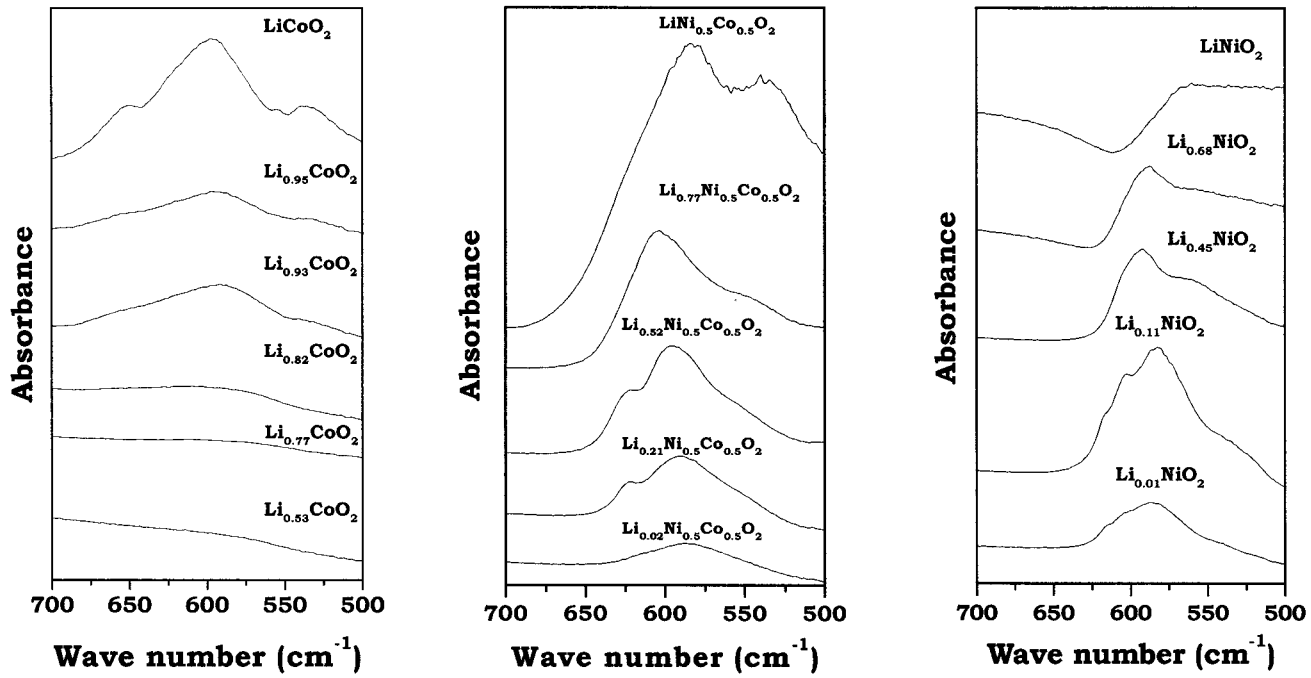

Figure 11. Infrared spectra of (a) $Li_{1-x}CoO_2$, (b) $Li_{1-x}Ni_{0.5}Co_{0.5}O_2$, and (c) $Li_{1-x}NiO_2$.

an oxygen content close to 2 with negligible amount of oxygen vacancies provide good structural stability to the nickel-rich phases and prevent the sliding of oxide-ion layers. Alternatively, a possible presence of a small amount of nickel in the lithium planes of the nickel-rich phases may also prevent the sliding as discussed before in the literature.[10−12]

In addition, the differences in the variation of *c* parameters with lithium content could also be explained by the observed differences in oxygen loss behavior. In the case of $Li_{1-x}CoO_{2-\delta}$, in-situ X-ray diffraction data[8] have shown that the *c* parameter increases initially with decreasing lithium content for $0.5 \leq (1 - x) \leq 1$, reaches a maximum at around $(1 - x) = 0.5$, and then decreases thereafter. On the other hand, the *c* parameter tends to increase with decreasing lithium content down to $(1 - x) \approx 0.2$ in the case of $Li_{1-x}NiO_{2-\delta}$[7] and $(1 - x) \approx 0.3$ in the case of $Li_{1-x}Ni_{0.8}Co_{0.2}O_{2-\delta}$.[25] The decrease in the *c* parameter at low lithium contents could be due to the formation of oxygen vacancies. The oxygen vacancies may lower the electrostatic repulsion between the oxide-ion layers and thereby decrease the *c* parameter. The formation of oxygen vacancies at an earlier stage in the case of $Li_{1-x}CoO_{2-\delta}$ leads to a decrease in *c* parameter at a higher lithium content compared to that in the nickel-rich phases.

Electrical Conduction. As the $Li_{1-x}Ni_{1-y}Co_yO_{2-\delta}$ samples are metastable and disproportionate at moderate temperatures of $T > 150$ °C, it is difficult to obtain sintered pellets that would be needed for direct resistivity measurements. However, a qualitative idea about the conduction process can be obtained by examining the infrared spectra of the samples. Accordingly, the infrared spectra of the $Li_{1-x}Ni_{1-y}Co_yO_{2-\delta}$ samples are shown in Figure 11 for $y = 0$, 0.5 and 1. In Figure 11, only the region corresponding to the bending and stretching modes of the $Ni_{1-y}Co_yO_6$ octahedra are shown. In the case of $Li_{1-x}CoO_{2-\delta}$ system, the intensity of the absorption bands decreases as the lithium content $(1 - x)$ decreases and the bands vanish completely for $(1 - x) < 0.77$. The vanishing of the bands signals a transition from a semiconducting behavior to a metallic behavior. As the electrical conductivity increases, the optical skin depth of the incident beam decreases, which leads to a probing of only the surface of the sample and a resulting decrease in the intensity of the absorption bands. Alternatively, when the sample becomes metallic, the free electrons are able to oscillate to any incident frequency resulting in no characteristic absorption. These results are consistent with the observation of metallic conductivity by Menetrier et al.[26] for $(1 - x) \leq 0.7$ in $Li_{1-x}CoO_{2-\delta}$. In contrast, the infrared spectra of $Li_{1-x}NiO_{2-\delta}$ and $Li_{1-x}Ni_{0.5}Co_{0.5}O_{2-\delta}$ exhibit bands even when all the lithium is extracted indicating a semiconductor behavior for the entire range of $0 \leq (1 - x) \leq 1$. Thus, the nickel-rich phases do not become metallic on extracting lithium.

The differences in the electrical conduction behavior can be explained on the basis of the qualitative energy diagram given in Figure 10. In the case of $LiCoO_2$ with a Co^{3+}:$3d^6$ configuration, a completely filled t_{2g} band leads to semiconducting behavior. As lithium is extracted, Co^{3+} is oxidized to Co^{4+} with an introduction of holes into the t_{2g} band. A direct Co−Co interaction through the partially filled t_{2g} bands across the shared octahedral edges along with a shortening of the Co−Co bond leads to metallic conductivity in $Li_{1-x}CoO_{2-\delta}$ for $(1 - x) < 0.77$. In contrast, a completely filled t_{2g} band for $0 \leq (1 - x) \leq 1$ in the case of $Li_{1-x}NiO_{2-\delta}$ leads to semiconducting behavior for the entire value of $(1 - x)$. Additionally, the Ni^{3+} ions are oxidized first before the Co^{3+} ions are oxidized since $Ni^{3+/4+}$:e_g band lies above

(25) Ronci, F.; Scrosati, B.; Albertini, V. R.; Perfetti, P. *Electrochem. Solid State Lett.* **2000**, *3*, 174.

(26) Menetrier, M.; Saadoune, I.; Levasseur, S.; Delmas, C. *J. Mater. Chem.* **1999**, *9*, 1135.

the $Co^{3+/4+}$:t_{2g} band as has been found before from electrical measurements and nuclear magnetic resonance studies.[27] This factor together with a lower oxidation state of the transition metal ions with oxygen vacancies (Figure 9) leads to semiconducting behavior for the entire value of $0 \leq (1 - x) \leq 1$ in $Li_{1-x}Co_{0.5}Ni_{0.5}O_{2-\delta}$.

Conclusions

$Li_{1-x}Ni_{1-y}Co_yO_{2-\delta}$ oxides have been synthesized by chemical extraction of lithium from $LiNi_{1-y}Co_yO_2$. The cobalt-rich phases tend to lose oxygen on deep lithium extraction due to an overlap of the $Co^{3+/4+}$:t_{2g} band with the top of the O:2p band. The nickel-rich phases, on the other hand, maintain an oxygen content close to 2 as the electrons are removed from the $Ni^{3+/4+}$:e_g band, which lies above the top of the O:2p band. The loss of oxygen in the cobalt-rich phases causes a sliding of the oxide-ion layers and a transformation of the initial O3 structure to P3 and O1 structures; nickel-rich phases maintain the O3 structure. While a completely filled t_{2g} band leads to semiconducting behavior in the nickel-rich phases for the entire $0 \leq (1 - x) \leq 1$, a partially filled t_{2g} band in $Li_{1-x}CoO_{2-\delta}$ leads to a semiconductor to metal transition around $(1 - x) \approx 0.77$. The tendency to lose oxygen limits the practical capacity of $LiCoO_2$ to 140 mAh/g (reversible extraction of 0.5 lithium per Co). On the other hand, the resistance to lose oxygen allows the realization of a higher practical capacity (180 mAh/g) for $LiNi_{0.85}Co_{0.15}O_2$. It should, however, be noted that neutral oxygen may not be evolved during an overcharge of lithium-ion cells made with $LiCoO_2$, but rather the cathode might undergo a reaction with the electrolyte. Although the nickel-rich cathodes exhibit better chemical stability than the $LiCoO_2$ cathode, they experience structural instability under mild heat due to a tendency of the Ni^{3+} ions to migrate to the lithium planes.[5] Additionally, a higher oxidation state of nickel in the charged state due to the larger capacity may have more safety problems compared to the cobalt oxide.

Acknowledgment. This work was supported by the Center for Space Power at the Texas A&M University (a NASA Commercial Space Center), Welch Foundation Grant F-1254, and Texas Advanced Technology Program Grant 003658-0488-1999.

CM0102537

(27) Saadoune, I.; Ménétrier, M.; Delmas C. *J. Mater Chem.* **1997**, *7*, 2505.